Filippo Stanco, Sebastiano Battiato, Giovanni Gallo

Digital Imaging for Cultural Heritage Preservation

Contributors

Sebastiano Battiato
University of Catania
Catania, Italy

Lamia Benyoussef
Ecole Centrale Marseille
Marseille, France

Simone Bianco
University of Milano Bicocca
Milan, Italy

Vittoria Bruni
Consiglio Nazionale delle Ricerche
Rome, Italy

Yang Cai
Carnegie Mellon University
Pittsburgh, USA

Roberto Caldelli
University of Florence
Florence, Italy

Marco Callieri
Consiglio Nazionale delle Ricerche
Pisa, Italy

Vito Cappellini
University of Florence
Florence, Italy

Paolo Cignoni
Consiglio Nazionale delle Ricerche
Pisa, Italy

Jacob Collins
c/o Adelson Galleries
New York, USA

Alessandro Colombo
University of Milano Bicocca
Milan, Italy

David Corrigan
Trinity College
Dublin, Ireland

Massimiliano Corsini
Consiglio Nazionale delle Ricerche
Pisa, Italy

Andrew Crawford
Consiglio Nazionale delle Ricerche
Rome, Italy

Paul Debevec
University of Southern California
Playa Vista, USA

Andrea Del Mastio
University of Florence
Florence, Italy

Andrey Del Pozo
Univesity of Illinois at Urbana-Champaign
Urbana, USA

Matteo Dellepiane
Consiglio Nazionale delle Ricerche
Pisa, Italy

Stéphane Derrode
École Centrale Marseille
Marseille, France

Gianpiero Di Blasi
University of Palermo
Palermo, Italy

Marco Duarte
Princeton University
Princeton, USA

Per Einarsson
University of Southern California
Playa Vista, USA

Marcos Fajardo
University of Southern California
Playa Vista, USA

Yasuo Furuichi
Kanagawa, Japan

Giovanni Gallo
University of Catania
Catania, Italy

Andrew Gardner
University of Southern California
Playa Vista, USA

Francesca Gasparini
University of Milano Bicocca
Milan, Italy

Tim Hawkins
University of Southern California
Playa Vista, USA

Andrew Jones
University of Southern California
Playa Vista, USA

Dave Kale
Stanford University
Stanford, USA

Anil Kokaram
Trinity College
Dublin, Ireland

Ashutosh Kulkarni
Stanford University
Stanford, USA

Therese Lundgren
University of Southern California
Playa Vista, USA

Philippe Martinez
Ecole Normale Superieure
Paris, France

Nikos Nikolaidis
Aristotle University of Thessaloniki
Thessaloniki, Greece

Ioannis Pitas
Aristotle University of Thessaloniki
Thessaloniki, Greece

Francois Pitie
Trinity College
Dublin, Ireland

Charis Poullis
University of Southern California
Playa Vista, USA

Giovanni Puglisi
University of Catania
Catania, Italy

Giovanni Ramponi
University of Trieste
Trieste, Italy

Fabio Remondino
B. Kessler Foundation (FBK)
Trento, Italy

Alfredo Restrepo Palacios
Universidad de los Andes
Bogotá, Colombia

M. Dirk Robinson
Ricoh Innovations
Menlo Park, USA

Silvio Savarese
University of Michigan
Ann Arbor, USA

Sara J. Schechner
Harvard University

Cambridge, USA

Raimondo Schettini
University of Milano Bicocca
Milan, Italy

Roberto Scopigno
Consiglio Nazionale delle Ricerche
Pisa, Italy

Ron Spronk
Queen's University,
Kingston, Canada

Filippo Stanco
University of Catania
Catania, Italy

David G. Stork
Ricoh Innovations
Menlo Park, USA

Jessi Stumpfel
University of Southern California
Playa Vista, USA

Davide Tanasi
University of Catania
Catania, Italy

Chris Tchou
University of Southern California
Playa Vista, USA

David Tingdahl
Katholieke Universiteit Leuven
Leuven, Belgium

Efthymia Tsamoura
Aristotle University of Thessaloniki
Thessaloniki, Greece

Christopher W. Tyler
Smith-Kettlewell Eye Research Institute
San Francisco, USA

Francesca Uccheddu
University of Florence
Florence, Italy

Luc Van Gool
Katholieke Universiteit Leuven
Leuven, Belgium

Maarten Vergauwen
GeoAutomation
Leuven, Belgium

Domenico Vitulano
Consiglio Nazionale delle Ricerche
Rome, Italy

Nathaniel Yun
University of Southern California
Playa Vista, USA

Nicholas C. Williams
Towan Headland
Cornwall, UK

Andrew R. Willis
University of North Carolina at Charlotte
Charlotte, USA

Silvia Zuffi
ITC CNR
Milan, Italy

Contents

16

Analysis of Ancient Mosaic Images for Dedicated Applications

Lamia Benyoussef and Stéphane Derrode

Institut Fresnel (CNRS UMR 6133)
École Centrale Marseille
Marseille, France
Email: lbenyoussef@ec-marseille.fr, sderrode@ec-marseille.fr

CONTENTS

16.1 Introduction

Mosaic is a form of art to produce decorative images or patterns out of small components. It requires a great deal of time and labor and it is often very expensive. Mosaic is, in return, far more durable in time than painting, so it can be used in places where painting cannot be of practical use, such as floors. Mosaic moreover allows the realization of light effects that are impossible with other media. The success of the mosaic art form through the ages is at the origin of large collections in several museums, among them we can cite the "Great Palace Mosaic Museum" (Istanbul, Turkey) and the "Musée du Bardo" (Tunis, Tunisia).

Recently, questions rise about the virtual conservation and management of collections and their accessibility to experts such as archeologists or art historians, and even to the large public. Requirements concern facilities

- for cataloging collections and distant consultation, and for intelligent retrieval tools (e.g., the extraction of objects with a semantic meaning, such as animal or human, in a complex mosaic scene);

- for virtual conservation (e.g., restoration of tesserae color), reconstruction (e.g., missing patches) and anastylosis of ancient mosaics.

The aim of this Chapter is to draw an overview of image processing based methods dedicated to the specificities of mosaic images for applications to restoration and cataloging of ancient mosaics.

16.1.1 Some Historical Facts about Mosaics

The following description only intends to give some basis entries about history of mosaics. And so, it is quite superficial and partial. Interested readers should consult the numerous books covering the subject, among them we can cite the following books [11, 16, 26]. The worldwide web gives also access to very complete lists of bibliographical references on ancient mosaics (e.g., [44]).

The earliest mosaics were installed as floors or pavements, occasionally as walls. Later, ceilings were also decorated. Originally, mosaics were used strictly in an architectural context. Mosaicking smaller, portable items such as panels or portraits is a later development, though there are a few rare instances of items such as icons from the late Byzantine era. The first mosaics that we know of are from what is now the Middle East. Temple columns in ancient Babylon (present day Iraq) had thousands of small clay cones pressed into wet plaster in decorative and geometric patterns. These date from five thousand years ago. From these humble beginnings, mosaic developed into a major art form. It was the Greeks, in the four centuries BC, who raised the pebble technique to an art form, with precise geometric patterns and detailed scenes of people and animals. By 200 BC, specially manufactured pieces "tessera" were being used to give extra detail and range of color to the work. Using small tesserae, sometimes only a few millimeters in size, meant that mosaics could imitate paintings. Many of the mosaics preserved at, for example, Pompeii were the work of Greek artists. The expansion of the Roman Empire took mosaics further afield, although the level of skill and artistry was diluted. Typically Roman subjects were scenes celebrating their gods, domestic themes and geometric designs.

With the rise of the Byzantine Empire from the $\mathbf{5}^{\boldsymbol{th}}$ century onwards, centered on Byzantium (present day Istanbul, Turkey), the art form took on new characteristics. These included Eastern influences in style and the use of special glass tesserae called "smalti", manufactured in northern Italy, made from thick sheets of colored glass. Smalti have a rough surface and contain tiny air bubbles. They are sometimes backed with reflective silver or gold leaf. Whereas Roman mosaics were mostly used as floors, the Byzantines specialized in covering walls and ceilings. The smalti were ungrouted, allowing light to reflect and refract within the glass. Also, they were set at slight angles to the wall, so that they caught the light in different ways. The gold tesserae sparkle as the viewer moves around within the building. Roman images were absorbed into the typical Christian themes of the Byzantine mosaics, although some work is decorative and some incorporates portraits of Emperors and Empresses.

In the west of Europe, the Moors brought Islamic mosaic and tile art into the Iberian peninsula in the $\mathbf{8}^{\boldsymbol{th}}$ century, while elsewhere in the Muslim world, stone, glass and ceramic were all used in mosaics. In contrast to the figurative representations in Byzantine art, Islamic motifs are mainly geometric. Examples can be seen in Spain at the Great Mosque at Cordoba, the *Alhambra Palace* and Meknes in Morocco (Figure 16.4(b)). In Arabic countries a distinctive decorative style called "zillij" uses purpose-made ceramic shapes that are further worked by hand to allow them to tessellate (fit together perfectly to cover a surface).

In the rest of Europe, mosaic went into decline throughout the Middle Ages, although some tiling patterns in abbeys, for example, used mosaic effects. In the $\mathbf{19}^{\boldsymbol{th}}$ century there was a revival of interest, particularly in the Byzantine style, with buildings such as Westminster Cathedral in London and *Sacre-Cœur* in Paris. The "Art Nouveau" movement also embraced mosaic art. In Barcelona, Antoni Gaudí worked with Josep Maria Jujol to produce the stunning ceramic mosaics of the *Guell Park* in the first two decades of the $\mathbf{20}^{\boldsymbol{th}}$ century. These used a technique known as *trencadis* in which tiles (purpose-made and waste tiles) covered surfaces of

buildings. They also incorporated broken crockery and other found objects, a revolutionary idea in formal art and architecture.

Mosaic still continue to interest artists but also crafts people because it is a very accessible, non-elitist form of creativity. The field is rich with new ideas and approaches, and organisations such as the British Association for Modern Mosaic (BAMM) [2] and the Society of American Mosaic Artists (SAMA) [1] exist to promote mosaic. As a recent example, we can cite the development of algorithms for computer-aided generation of mosaic images from a raster image, simulating ancient or modern styles [6].

16.1.2 Mosaics, Images and Digital Applications

Mosaics are made of colored tiles, called tessera or tessella, usually formed in the shape of a cube of materials separated by a joint of mortar. The earliest known mosaic materials were small cones of clay pressed into wet plaster. Semi-precious stones such as lapis lazuli and onyx, as well as shells and terra cotta were also used. As the art developed, glass, ceramic and stone tesserae were the most common materials, along with pebbles. Modernly, any small singular component can be used: traditional materials, glass or ceramic cast or cut into tiles, plus plastic, polymer clay (such as Sculpey or Fimo), beads, buttons, bottle caps, pearls, etc. The physical study of materials used in mosaics continue to be an active research field [10, 17, 38].

Structure characteristics

Mosaics can be built on different natural ground made of soil or rock, or on top of a previous pavement. The mosaic itself is composed of a variety of foundation or preparatory layers and a layer of tesserae. Also, the mosaic surface exhibits irregular hollows (tesserae) and bumps (mortar) through the scene. Hence, a mosaic can not be considered as a plane surface, as for paintings, but has numerous forms of irregularities, typical of the artwork style:

- *Shape of tesserae*, The shapes of tesserae are irregular, from square shapes to polygonal ones.
- *Organization of tesserae*, Tesserae are not positioned according to a regular lattice. On the contrary, the smart and judicious choice in the orientation, size and positioning of tesserae characterize the artwork style and exhibit the "general flow" (guidelines) of the mosaic chosen by the mosaicist.
- *Mortar joint*, This positioning makes the joints appear as an irregular network with numerous interconnections throughout the mosaic. Network color intensity, mainly middle gray, is however not uniform through the scene.
- *Color of tesserae*, Because of materials used and their oldness, tesserae of ancient mosaics are generally characterized by pastel colors, with low contrast.

Oldness characteristics

Other artifacts can be associated to the wear, erosion and oldness of ancient mosaics (some of them are illustrated by images in Figures 16.1 and 16.2):

- *Disaggregated tesserae*, Some tesserae can display a loss of cohesion of their surfaces, disintegrated into powder or small grains. Also erosion and patinae deteriorations are commonly encountered in studying ancient mosaics.
- *Missing tessera patches*, Most of mosaics are not completely preserved and, as a consequence of disaggregation, lacunas generally corrupted mosaic scenes.
- *Color alteration*, Alteration of the mosaic surface characterized by a localized change in color (due to fire damage, graffiti, etc.).

FIGURE 16.1
Excerpt of an ancient Greek mosaic scene (from Paphos, Cyprus), showing missing patches and geometric deformation due to slant acquisition [25], public domain image.

(a) Disaggregated (b) Eroded (c) Altered in color

FIGURE 16.2
Three examples of deteriorated tesserae, from [34].

Data acquisition

For latter processing and virtual anastylosis, mosaic scene must first be digitized using camera. All peculiarities cited above have a strong and complex impact on acquisition and the way mosaic scenes appear in an image with a limited resolution:

- *Relief shadows*, During snapshot acquisition, the relief of tesserae generates shadows on mortar which does not appear nearly uniform in intensity all over the image, as it should be.
- *Indoor/outdoor acquisition*, Previous item is further accentuated by indoor acquisition with flash. In outdoor acquisition, light is not controlled and one should expect severe contrast variations in acquisitions.
- *Geometric deformation*, Another degradation comes from the snapshot acquisition angle, especially for very large mosaic scenes lying on the floor. This point produces perspective (rotation, scaling and shearing) deformations of tesserae shape in image and the thinning down of the mortar width (till disappearing).
- *Tessera resolution*, The resolution of tesserae in an image (i.e., the number of pixels to describe a tessera) should not be too low for latter processing. On the other hand, a too high resolution will only able to capture partial scene.

As a consequence, very large mosaic scenes have to be recorded using multiple overlapping images that are subsequently co-registered in geometry and color to produce the entire digital scene. An interesting complementary approach to camera acquisition is given by laser scanning. This technique, used recently for ancient mosaics analysis [23, 37], can produce a 3D mesh of the mosaic surface and material for a detailed shape analysis.

Hence, dedicated processing methods are required to take into account the specificities of mosaic and the specificities of mosaic images, and to adopt image processing strategies suited to the tiling organisation of tesserae. This way, one can expect better performances than general purpose algorithms. The nature and the artifacts in mosaic images make segmentation methods based on pixel intensities inefficient (e.g., pixels associated to the mortar interfere with the classification process of tesserae). A strategy better suited to mosaic images is to consider tesserae as indivisible entities with an almost uniform gray-level value.

The remaining of the Chapter starts in Section 16.2 with a brief description of several projects involving image processing methods for restoration, preservation and indexation of ancient mosaics. Then we present in details some fondamental applications of the tessera-oriented point-of-view on mosaic images proposed by the authors, according to the diagram in Figure 16.3. Section 16.3 presents an effective way to extract tesserae, while Section 16.4 exposes two direct applications of this strategy for mosaic image segmentation and coding. Section 16.5 presents an effective way to retrieve the main guidelines of a mosaic which can be helpful for delimitating semantic objects present in a complex scene. Finally, the conclusion in Section 16.6 examines some open issues and suggests future research directions to succeed in providing appropriated tools to museums and experts.

16.2 Recent Image Processing Projects Concerned with Mosaics

A few project involving computer science and image processing for mosaic conservation, restoration or cataloging are reported in the literature. Here is a short description of them.

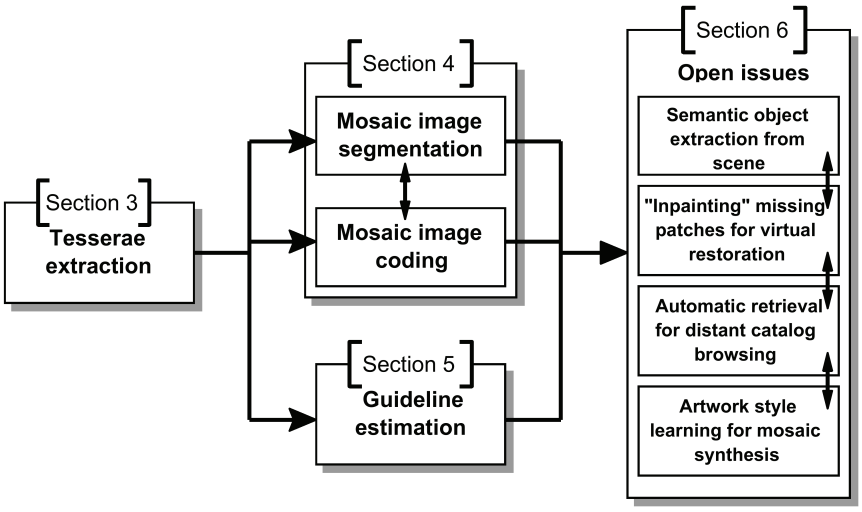

FIGURE 16.3
Organization of Chapter with the processing pipeline.

16.2.1 St. Vitus Cathedral Mosaic Restoration

The more accomplished project concerns the restoration of the St. Vitus cathedral mosaics, in Prague (Czech Republic), reported in [49]. The Golden Gate (the southern entrance to the cathedral) is decorated with a unique work of art: a colored, richly gilded mosaic representing the Last Judgement, see Figure 16.4(a). In 1992 the Office of the President of the Czech Republic and the Getty Conservation Institute [3] began to cooperate to restore and conserve the mosaic.

Having the historical photo of the mosaic from the end of the $\mathbf{19}^{th}$ century and the photos of the current state, authors study the evolution of the mosaic, which was several times reconstructed and conserved. Firstly they tried to restore the historical photograph - remove noise , deblur the image, increase the contrast. Then, they remove the geometrical difference between images by means of the multi-modal registration using mutual information. Finally, they identify mutual differences between the photos, which indicate the changes on the mosaic during the centuries.

16.2.2 Arabo-moresque and Islamic Mosaic Pattern Classification

Lot of attention has also been paid to islamic mosaics, of which artwork style is illustrated through Figure 16.4(b). The particularities of such mosaics come from the periodicity and symmetry of tile patterns.

A. Zarghili *et al*, [47, 48] propose a method to index an Arabo-Moresque decor database which is not based on symmetry. They use a supervised mosaicking technique to capture the whole principal geometric information (connected set of polygonal shapes, called “spine”) of a pattern. The spine is then described by using Fourier shape descriptors [35] to allow retrieving of images even under translation, rotation and scale. But, according to [14], the method cannot be automatized and does not allow the classification of these patterns according to any criterion.

In [21], the authors propose image processing techniques to restore mosaic patterns. Image analysis tools are developed to obtain information about design patterns which are used to recover missing motifs or

(a) (b)

FIGURE 16.4
(a) Photo of the "Last Judgement" mosaic in the St. Vitus cathedral (Prague, Czech Republic), from [4]. (b) Islamic mosaic (Meknes, Morocco).

tesserae. One difficulty was to propose methods robust to the discrepancies between equal object shapes (due to manual artwork, oldness, etc.). The symmetry, once recovered, allows virtual reconstruction by inpainting methods and physical restoration of damaged parts of mosaics.

To study Islamic geometrical patterns, and all periodic patterns such as those encountered in textile patterns [41] or wallpapers, several works are based on the symmetry group theory. In [14], authors first classify patterns into one of the three following categories: (i) pattern generated by translation along one dimension, (ii) patterns which contain translational symmetries in two independent directions (refers to the seventeen wallpaper groups), and (iii) "rosettes" that describes patterns which begin at a central point and grow radially outward. For every pattern, authors extract the symmetry group and the fundamental region (i.e., a representative region in the image from which the whole image can be regenerated). Finally, they describe the fundamental region by a simple color histogram and build the feature vector which is a combination of the symmetry feature and histogram information. Authors shows promising experiments for either classification or indexing.

In [15], authors exploit symmetry and auto-similarity of motifs to design a system to index Arabo-Moresque mosaic images based on the fractal dimension. Mosaics are first segmented automatically using color information. The classification decomposes the initial motif into a set of basic shapes. Contours of those shapes are then characterized by their fractal dimension which gives, according to the authors, a relevant measure of the geometric structure of the tile pattern. Some retrieval performances are also reported.

16.2.3 Roman Mosaics Indexation

Recently, two Content-Based Image Retrieval (CBIR) systems have been proposed to catalog and index Roman mosaic images.

The first one, proposed in [32], details a complete CBIR system which include (i) object extraction from a complex mosaic scene by using unsupervised statistical segmentation and (ii) invariant description of semantic objects using the analytical Fourier-Mellin transform [13, 20]. Similarity between querying mosaic and the database is based on an index constructed from the invariant descriptors and an appropriate metric (Euclidean and Hausdorff).

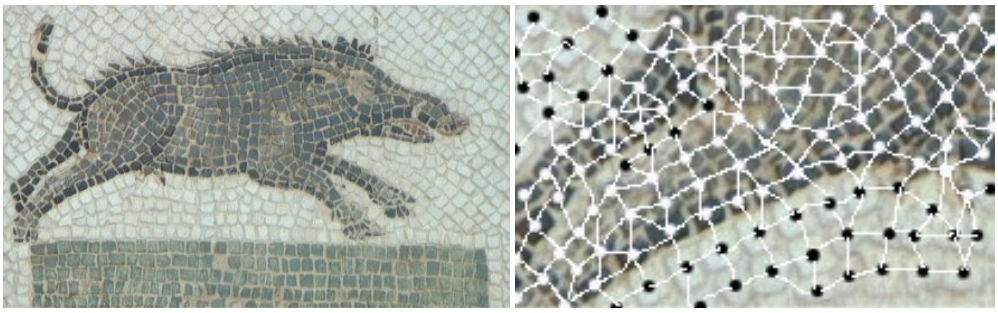

(a) (b)

FIGURE 16.5
Excerpt of an ancient mosaic showing a wild boar (a) and a zoom on its hind legs (b).

The second CBIR [27, 28] is a general system to index and retrieve by the content historic document images. While the object annotation in database images is done manually and off-line, the indexation is done automatically using an extended curvature scale space descriptor [33] suitable for concave and convex shapes. The query/retrieval of pertinent shapes from the database starts with a user drawing query (with a computer mouse or a pen) that is compared to entries in the database using a fuzzy similarity measure. The system integrates an XML Database conform to the MPEG7 standard, and experiments on large databases providing by the National Library of Tunisia and some Tunisian museums are reported.

One key-point for such systems to be effective is to improve semantic objects extraction. Pixel-based methods, as the one used in [32], require heavy post-processing to detect shapes of interest from pixels classe. Recently, a new viewpoint on mosaic images, based directly on tesserae, have been proposed [8]. Once tessera extraction is achieved, this strategy facilitates basic steps toward CBIR applications, as described in the following.

16.3 Tesserae Extraction

A "natural way" to describe mosaics is to consider tesserae in their own instead of groups of isolated pixels, allowing to develop tessera-oriented processing. Indeed, a mosaic image can be seen as an irregular lattice in which a node is a tessera (Figure 16.5). The grid structure has been superposed to the zoomed image in Figure 16.5(b) to illustrate the complexity of the neighborhood system, both in the number of neighbors and in their orientation. To adopt this point of view on mosaic images, a robust method is required to extract tesserae from the network of mortar surrounding them.

A way to consider this problem is to deal with the dual problem (i.e., the extraction of the network of mortar) which is close to recurrent problems encountered in several image processing applications (i.e., in medical imaging: vascular network segmentation from angiographies [12, 46], or in satellite imaging: road extraction in urban scenes [29, 30]).

Several approaches have been proposed. Methods based on contour extraction are widely used and mainly

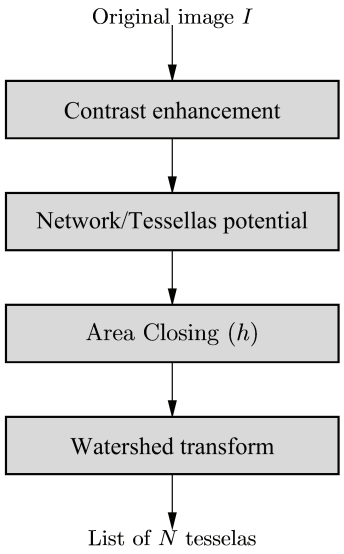

FIGURE 16.6
Processing chain involved in tessera extraction, using gray-scale morphology tools.

rely on the assumption that the network pixels and neighboring ones have different gray levels in order to compute gradients. But methods based on high-pass filter, such as Harris's corner detector, highlight pixels belonging to the network, not connected components. Higher-level processings detect lines with varying widths [18, 39]. Strategies that track the entire network from a starting point [7, 45] are difficult to justify in the mosaic image case due to the high number of interconnections in a mosaic network graph.

Numerous methods based on Markov modeling [19,40] or active contours [36,42] have also been proposed. These methods are quite efficient but time consuming. In the case of mosaics, these methods are not suited because of the high density of the network to be extracted in images. In [19], a Markov model is applied on a graph of adjacency crests, detected by a Watershed Transformation applied on a criterion image. This criterion image, computed from the original one, exhibits the potential of each pixel to belong to the network.

A study of tessera extraction has been conducted in [8]. The solution adopted, and preferred over other experimented strategies, is based on gray-level morphology which is suited to the tiling organisation of mosaics. The Watershed Transformation (WT) approach [31] appeared interesting for mosaic images since this method is a good compromise between low-level methods (contour detection) and approaches by energy minimization (Markov model or active contours). But to work well, the WT needs to be computed on a criterion image (processed from the original one) that shows tesserae as catchment basins and the mortar network as watershed crests.

The entire algorithm is sketched in Figure 16.6. The goal is to present to the WT a potential image that exhibits tesserae as catchment basins and the network as a crest crossing the entire image. The pre-processings are: (i) Contrast enhancement, based on top-hat and bottom-hat transforms; (ii) Potential criterion computation to exhibit the network as a crest; and (iii) Area closing [43] to reduce over-detection by WT.

The extraction quality highly depends on the way mosaic images have been acquired. It should be taken not too far from the mosaic since individual tiles will not be visible: according to experiments, tesserae should appear with a resolution of not less than $\mathbf{10} \times \mathbf{10}$ pixels. Parameter $\boldsymbol{h}$ is a threshold used by the area closing

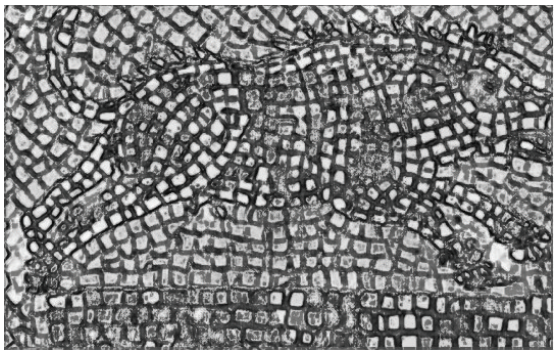

FIGURE 16.7
Criterion image obtained from Figure 16.5. This processing improves the contrat between tessera and the network of mortar.

operator [43]. Its value has an impact on the number of extracted tiles: a small value gives an over-detection whereas a big one produces an under-detection one. Hence, it should be (roughly) adjusted according to the mean size α of tesserae in the image (in number of pixels), assuming that α almost constant in a mosaic. Parameter h should be less than α^2 to avoid small tesserae to be deleted by the morphological operator. In experiments, value $h = \alpha^2/2$ gives good results.

Figure 16.7 shows the criterion image obtained by applying the method to the wild boar image. As can be seen in this example, the network appears in dark. However tesserae are not uniform in texture and show local gray-level crests that should be deleted before WT in order to avoid over-segmentation. Following [19], an area closing [43] in first computed on the criterion image. This processing gives fewer minima while retaining crest locations as illustrated in Figure 16.8. The crest contours now represent correctly the network, which is confirmed by the zoom in Figure 16.9(a). To determine the width of the network (and not only a one-pixel skeleton as done by WT), which varies through the image, a simple threshold is applied on neighboring pixels of crests: a pixel is aggregated to the crest if its gray value is no more different by 10% of the skeleton mean gray value. The result of applying such a threshold can be observed in Figure 16.9(b).

A second example of tessera extraction based on gray-level morphological processing in given in Figure 16.10.

16.4 Tessera-based Segmentation and Coding

This Section describes two simple and direct applications of the tessera-oriented representation of ancient mosaic images: segmentation and coding. Especially, these applications preserve the irregularity of tiles shape and so the mosaic effect perception. From now, we assume that all tesserae in a mosaic image have been extracted successfully (i.e., one can access the coordinates of every pixel belonging to the contour of each tile in the mosaic). Each pixel that does not belong to a tessera is assumed to be a background pixel (i.e., a mortar network pixel).

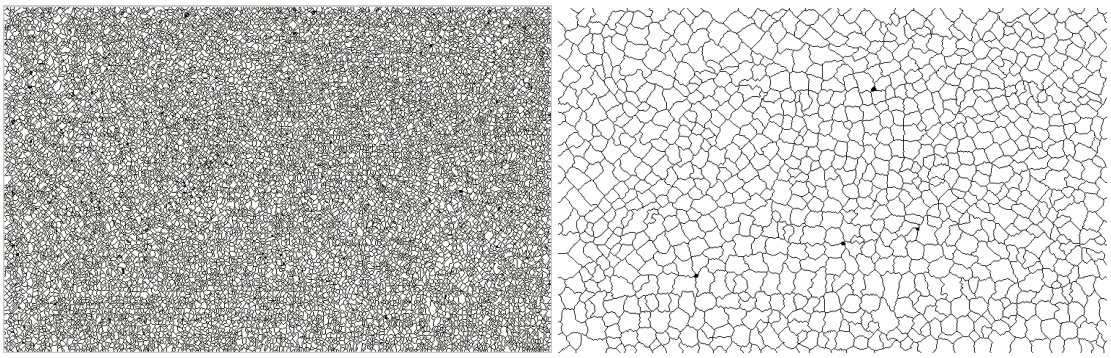

(a) (b)

FIGURE 16.8
Extraction of tesserae from the criterion image in Figure 16.7, without (a) and with (b) area closing operator.

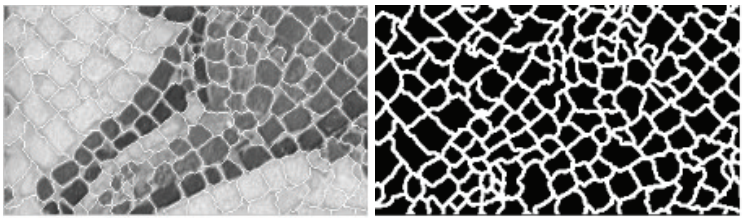

(a) (b)

FIGURE 16.9
Result of tessera extraction on the zoom in Figure 16.5(a) in (a), and network/tesserae classification in (b).

(a) (b)

FIGURE 16.10
Illustration of the tessera extraction algorithm on the mosaic image of a Deer.

16.4.1 Segmentation of Ancient Mosaic Images

Instead of using all pixels from the tesserae, and since tesserae are almost homogeneous in color, classification can be performed directly on tesserae, not on pixels, by using some dedicated features. Tesserae can be characterized by several features, among them the mean and variance of gray-level values. Also one can take into account the number of pixels in the tessera, using a multi-features classification. All pixels belonging to the mortar network are directly associated to a unique class (they do not participate to the classification). The class color corresponds to the mean color of the mortar pixels.

In Figure 16.11, a simple K-means algorithm based on the mean gray-level value of tesserae was sufficient to get an interesting segmentation. From a semantic point of view, this segmentation outperforms the result obtained by a classical pixel-based K-means strategy. A second example that confirms such interesting behavior is provided in Figure 16.12. Once again, the segmentation quality depends on the robustness of tessera extraction.

16.4.2 Tessera-based Coding and Lossy Compression

Another direct application of the WT tessera labeling is to develop a compact and efficient coding representation of ancient mosaic images [9]. This kind of module can be useful for rapid thumbnails transmission in case of distant catalog browsing application. The compression proposed is lossy but preserves the specificities of mosaic images, especially the irregularity of tesserae shape. In a way, the strategy described below is better suited to ancient mosaic images than a general purpose lossy compression algorithm, such as `jpeg` which is based on square-blocks.

We still consider that all tesserae in a mosaic have been extracted successfully (i.e., we can access the coordinates of every pixel belonging to the contour of each tile in the mosaic). The network can be seen as the mosaic image background (i.e., each pixel that does not belong to a tessera is assumed to be a background pixel). Let $\boldsymbol{I}$ be a mosaic image with dimensions $\boldsymbol{L} \times \boldsymbol{C}$, made of $\boldsymbol{N}$ colored tiles. The tessera-based lossy-compression specificity has been designed in order to take into account the two following observations:

- A tile $\boldsymbol{n}$, $\boldsymbol{n} \in [\mathbf{1}, \boldsymbol{N}]$, is usually formed in the shape of a cube of material, mostly with uniform color.

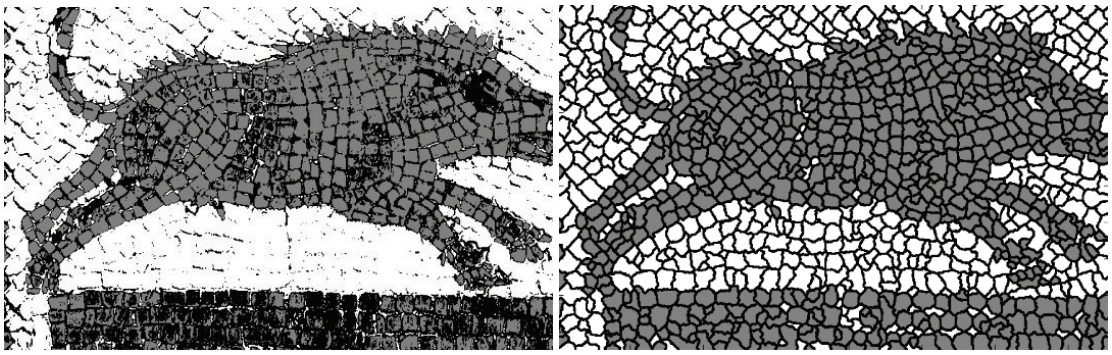

(a) Pixel-based K-means segmentation (b) Tile-based K-means segmentation

FIGURE 16.11
Segmentation comparison of the mosaic image in Figure 16.5(a) with a pixel-based strategy (a) and the tessera-based strategy presented in Section 16.3 (b). Both pixel- and tile-based segmentations make use of an unsupervised K-means classification algorithm, the first one with 3 classes, and the second one only with 2 classes since the mortar is already extracted.

Hence a vector of three intensity colors $(\boldsymbol{R_n}, \boldsymbol{G_n}, \boldsymbol{B_n})$ is enough to describe the color of tessera $\boldsymbol{n}$. This color can be easily estimated by computing the mean intensity of pixels belonging to the tessera.

- The mortar intensity, mainly middle gray, is not uniform throughout the image because of shadows due to non-flat mosaic surfaces and snapshot acquisition angle. However, the network intensity should appear the same everywhere in the image. Hence, all pixels belonging to the mortar network is coded by the same color vector $(\boldsymbol{R_b}, \boldsymbol{G_b}, \boldsymbol{B_b})$, $\boldsymbol{b}$ stands for *background*. This value can be estimated by computing the mean intensity of network.

Coding file structure
The `cms` ("Compressed MoSaic") format is structured as follows (see Figure 16.13) :

- **Header:** The header is made of

  1. The original image size in pixels ($\mathbf{2} \times \mathbf{2}$ bytes).
  2. The number $\boldsymbol{N}$ of tesserae in the image (2 bytes).
  3. The mean color values $(\boldsymbol{R_b}, \boldsymbol{G_b}, \boldsymbol{B_b})$ of the network (3 bytes).

  Hence, nine bytes are necessary to code the header. Other information such as the name of the original image or a comment can be added.

- **Body:** each tessera $\boldsymbol{n}$ has the following code structure

  1. *Tessera header* contains the number of pixels $\boldsymbol{N_n}$ of the contour (1 byte), and the mean color values $(\boldsymbol{R_n}, \boldsymbol{G_n}, \boldsymbol{B_n})$ of the tessera (3 bytes).

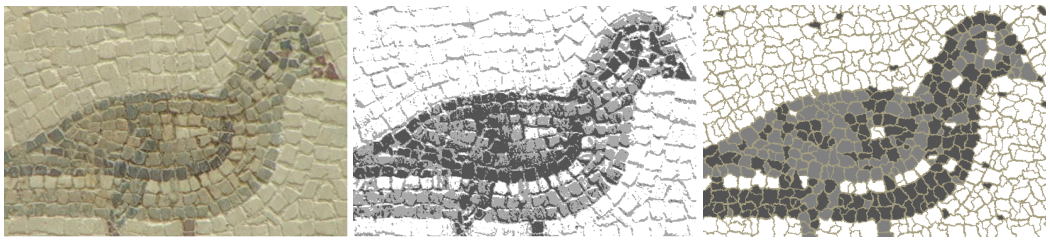

(a) (b) (c)

FIGURE 16.12
K-means segmentation of a mosaic representing a bird (a) with the pixel-based (b) and the tile-based (c) strategies.

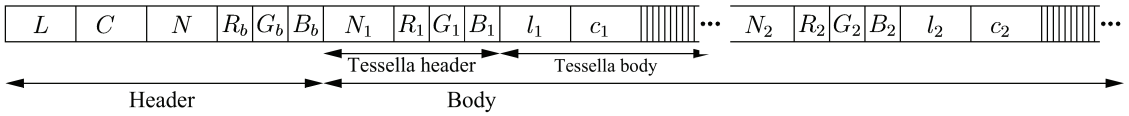

FIGURE 16.13
Sketch of the `cms` file format to compress images of ancient mosaics (without Huffman coding).

2. *Tessera body* codes the closed-contour using the coordinates $(\boldsymbol{l_1},\boldsymbol{c_1})$ of the first pixel ($\mathbf{4}$ bytes) and Freeman chain code (or whatever code) for the subsequent $\boldsymbol{N_n - 1}$ pixels. If no Huffman coding technic is applied, only 3 bits per contour pixels are necessary.

Counting the number of bytes necessary to code a tessera $\boldsymbol{n}$ gives: $\mathbf{8} + \frac{(\boldsymbol{N_n}-\mathbf{1})\ \mathbf{3}}{\mathbf{8}}$ rounded to the ceil value. The last byte is filled in to start the next tessera coding on a new byte. Hence, 21 bytes are needed to code a tessera with $\boldsymbol{N_n} = \mathbf{34}$.

Mosaic image reconstruction from the compressed file is done by reconstructing the image background using the network color intensity, on which each tessera with its own color is superposed. The order tesserae are saved or read in the body of the `cms` file has no influence on the reconstruction quality, but can be changed for a desired application. For example, one can think organizing tesserae by grouping tiles in the file according to the semantic object they belong to (e.g., human, animal, etc.). Hence reconstruction will progressively show the different objects present in the mosaic scene. Tesserae dedicated to the background, mainly of uniform color as illustrated in Figures 16.5(a), 16.10(a) and 16.12(a), can be saved at the end of the file since their semantic meaning is, in general, less interesting than the one from objects tesserae. Specific organization of tesserae within the file can also be of interest for mosaic database indexing and text- or content-based retrieval, see Section 16.6. Hence, we get a compact and easy-to-handle lossy-compressed representation of mosaic image. The compression of a mosaic image and its reconstruction from a `cms` file are summed up in Algorithms 1 and 2.

Experimental results

To evaluate the compression algorithm, we process on the Deer mosaic image in Figure 16.10(a). The decoding result is shown in Figure 16.14 and must to be compared with the original image. Pixels attributed

Algorithm 1 `cms` format coding.

Require: Mosaic image $\boldsymbol{I}$.
Ensure: Tessera-oriented coding of $\boldsymbol{I}$ in file `f`.
  Tessera extraction (*cf.* Section 16.3).
  for $n = 1, \ldots, N$ **do**
    Write the number of contour pixels $N_n \leftarrow$ `f`.
    Write the mean color value $V_n \leftarrow$ `f`.
    Write the first contour pixel coordinates $l_n, c_n \leftarrow$ `f`.
    for $i = 2, \ldots, N_n$ **do**
      Compute chain code direction for pixel i.
      Write direction $\leftarrow$ `f`.
    end for
  end for

Algorithm 2 `cms` format decoding.

Require: Compressed file `f`.
Ensure: Tessera-oriented decoding of file `f` into image $\boldsymbol{I}$.
  Read file header $\rightarrow L, C, N, R_b, G_b, B_b$.
  Create an image $\boldsymbol{I}$ with dimensions $L \times C$ and background color (R_b, G_b, B_b).
  for $n = 1, \ldots, N$ **do**
    Read tessera header $\rightarrow N_n, R_n, G_n, B_n, l_n, c_n$.
    Set pixel (l_n, c_n) with color (R_n, G_n, B_n).
    for $i = 2, \ldots, N_n$ **do**
      Compute coordinates (l_i, c_i).
      Set pixel (l_i, c_i) with color (R_n, G_n, B_n).
    end for
    Fill in the closed contour with color (R_n, G_n, B_n).
  end for

FIGURE 16.14
Result of coding/decoding of the Deer image in Figure 16.10(a).

to the network represent $\mathbf{27.5\%}$ of the total number of pixels in the image ($\mathbf{255 \times 394}$). The number of tesserae detected is 314. The image produces a `cms` file size of $\mathbf{8766}$ bytes, which gives a compression factor of about $\mathbf{11.5}$ with respect to a raw coding of pixels (e.g., `ppm` file format). The compression ratio depends on the mean tessera size in the mosaic image. The bigger the tiles, the higher the compression ratio is expected to be.

From a qualitative point of view, some remarks can be pointed out. As expected the shape of the network and tesserae is kept very similar to the original ones. The mean colors used to describe network and tesserae intensities makes the decoded image appears pastel with respect to the original one, since artifacts such as shadow or dirties are cleaned. Nevertheless the global aspect of the mosaic is respected and of sufficient quality to understand the scene content. Lacunas and missing patches are not taken into account by the actual algorithm. It considers holes as tesserae but should better associate them to the mortar network since we observe the preparatory layer mortar appears behind. One solution is to fuse the network with tesserae that show mean color close to the mean network color.

16.5 Guidelines Estimation for Mosaic Structure Retrieval

Ancient mosaicists avoided to align their tiles according to rectangular grids. Indeed, such grids emphasize only horizontal and vertical lines and may distract the observer from seeing the overall picture. Hence, they placed tiles in order to emphasis the strong edges of the subject to be represented, influencing the overall perception of the mosaic [5]. Hence, organization and positioning of tesserae are interesting information for experts since they emphasize the main directional guidelines chosen by the artist (characteristic of the style). This information is of crucial interest for mosaic dedicated applications such as content-based retrieval of semantic elements or region-based mosaic image coding.

To get directional guidelines, one can first think using the principal axes of an ellipse-equivalent shape of each tessera, using well-known formulae based on geometrical moments (minor and majors axes). However, ancient mosaic tesserae are not box- neither regular-shaped and principal axes quickly appear not enough robust. One major drawback of such method is that it does not take into account information of neighboring tesserae, which is of great importance for regularization and for recovering the main guidelines that emphasize the "general flow" of a mosaic.

Hence, an energy-based contextual algorithm for retrieving main directional guidelines in a mosaic has been proposed [8]. The energy to be minimized is constructed by using two key-features: the mean-gray value and borders directions of each tessera. The optimization is done either by gradient descent or by simulated annealing.

Methodology

Each tessera $\boldsymbol{n}$ is represented by

- Its barycenter $(\boldsymbol{x_n}, \boldsymbol{y_n})$ computed on the support $\boldsymbol{\Omega_n}$ of $\boldsymbol{n}$.
- The list of its neighboring tesserae: $\boldsymbol{\mathcal{V}_n} = \{\boldsymbol{v_{n,1}}, \ldots, \boldsymbol{v_{n,T_n}}\}$. A neighbor is a tessera that shares at least one pixel of mortar network with $\boldsymbol{n}$.

It should be noted that the number of neighbors $\boldsymbol{T_n}$ is different from one tile to the other since tesserae are not organized according to a regular grid. Each tessera $\boldsymbol{n}$ is characterized by an energy of configuration which links itself to each of its neighbor $\boldsymbol{v_{n,t}} \in \boldsymbol{\mathcal{V}_n}$. This energy, denoted by $\boldsymbol{E_{n,t}}$ with $\boldsymbol{t} \in [\mathbf{1}, \ldots, \boldsymbol{T_n}]$, is the sum of two complementary terms:

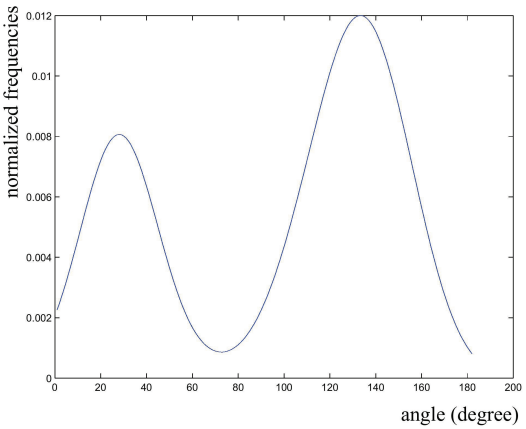

FIGURE 16.15
Plot of the regularized and normalized histogram of the contour orientation of one tile from the boar mosaic image in Figure 16.5(a).

- The first term $\boldsymbol{Q}$ is based on the mean-gray value of tesserae. It is proportional to the sum of the difference of gray-level means (1) between $\boldsymbol{n}$ and $\boldsymbol{v_{n,t}}$, and (2) between $\boldsymbol{n}$ and the symmetrical tessera of $\boldsymbol{v_{n,t}}$ with respect to $\boldsymbol{n}$. This feature favors alinement of tesserae with low contrast, which is a characteristic of directional guidelines.
- The second term $\boldsymbol{R}$ is based on the orientation of tessera contours. We compute the histogram of the orientation of segments constituting the contour of tessera $\boldsymbol{n}$. This histogram is regularized using a Gaussian kernel, result of which is illustrated in Figure 16.15. It should be noted that the two modes of the histogram, at approximatively $\mathbf{90^0}$ each other, correspond to the two ambiguous orthogonal main directions of a square-shaped tile. It is then possible to estimate the p.d.f. at angle $\boldsymbol{\alpha_{n,t}}$ given by the barycenter of $\boldsymbol{n}$ and the one of $\boldsymbol{v_{n,t}}$.

Terms $\boldsymbol{Q}$ and $\boldsymbol{R}$ are normalized to belong to range $[\mathbf{0}, \mathbf{1}]$. We can then initialize the "main direction" of a tile (i.e., the direction of the neighboring tessera which gives the highest $\boldsymbol{Q} + \boldsymbol{R}$ value):

$$\boldsymbol{t_{n,max}} = \mathbf{arg} \max_{t \in [1,\ldots,T_n]} \boldsymbol{E_{n,t}} \tag{16.1}$$

The energy of a tessera is then defined as $\boldsymbol{C_n} = (\mathbf{2} - \boldsymbol{E_{n,t_{n,max}}}) + \boldsymbol{\lambda}\, \boldsymbol{V_n}$, with $\boldsymbol{\lambda}$ a weighting factor set manually. Term $\boldsymbol{V_n}$ is defined as

$$\boldsymbol{V_n} = \frac{\mathbf{1}}{\boldsymbol{T_n}} \sum_{t=1}^{T_n} \left| \boldsymbol{\alpha_{n,t_{n,max}}} - \boldsymbol{\alpha_{t,t_{t,max}}} \right| \tag{16.2}$$

which is the normalized sum of absolute difference between the main direction of tile $\boldsymbol{n}$ and the main direction of its neighbor $\boldsymbol{t}$.

The next step to to minimize the mosaic energy, defined as the sum of $\boldsymbol{C_n}$ for all tesserae in the mosaic. This is done by selecting the tessera $\boldsymbol{n}$ which gives the highest value for $\boldsymbol{V_n}$. To reduce the contribution of this tessera, we try another main direction and recompute the mosaic energy. At that point, two strategies have been tested:

- Deterministic framework (Gradient Descent): if the mosaic energy reduces then the new main direction is validated, otherwise another main direction is tested. When all directions for this tile have been tested, we repeat the process for the next tile with high V_n value.

- Stochastic framework (Simulated Annealing): a configuration which gives a higher mosaic energy can be validated according to the simulated annealing principle [24]. This strategy allows to search for the global minimum, which can not be reached with previous strategy since the mosaic energy function is not convex.

The process is iterated until the mosaic energy is almost constant. The cartography of tessera orientation is made of the main direction of each tile at the last iteration.

Figure 16.16 illustrates the application of the tessera orientation methodology on the detail of the boar image in Figure 16.5(a). From the initial configuration of tesserae (a) we get the final configuration (b) using Simulated Annealing (SA) for optimization. Figure 16.16(c) shows the evolution of the computed energy during iterations of both gradient descent (GD) algorithm and simulated annealing one. As expected, SA reaches a lower minimum than GD but to the detriment of numerous additional iterations (approximately 150 for SA versus 50 for GD). Indeed, GD searches for a local minimum and is highly dependent on the initial configuration, whereas SA is expected to reach the global minimum due to its stochastic nature.

The tessera cartography obtained with SA optimization is really satisfying when visually compared to the main directional guidelines of the mosaic. This is especially true for regions at the borders between classes. A second example of cartography is proposed in Figure 16.17, after both simulated annealing and gradient descent optimizations. Results are very similar except for some guidelines where SA gives a better result. Once again, the tessera orientation estimation methodology, which makes use of contextual information, gives regularized results that emphasize the mosaic guidelines. Nevertheless, confusions can be found on areas with homogeneous colors and where tesserae are square-like shaped. Indeed, for those kinds of tesserae two orthogonal directions are equally probable, which generally gives ambiguous results. However, these areas of uniform color are of limited interest for object-based scene applications, such as mosaic pattern recognition.

Finally, Figure 16.18 shows a failure case in tessera orientation estimation. Indeed, the result will not allow to find the main directional guidelines in the mosaic, that can be more easily observed in Figure 16.12(a). The main reason comes from an over-detection of tesserae from the extraction step. This behavior is observed on mosaics built with tesserae of different sizes (*e.g.* large tesserae for the background and small ones for objects or details). Hence the shape of extracted tiles does not correspond to the shape of tesserae and the orientation is corrupted, showing no particular guideline in the mosaic.

16.6 Open Issues and Research Directions in Mosaic Image Analysis

In this Chapter, an overview of image processing methods for images of ancient mosaics has been proposed. The analysis of such images is a difficult task due to many reasons, among them the irregularity of shapes, the particular organization of tesserae and the degradation of tiles due to their oldness. Also, the way snapshot acquisition is performed has a crucial impact on the subsequent processings.

A few works only are reported in the literature regarding the numerous problems that experts (museum curators, archeologists, art historians, etc.) face about possibly virtual restoration/lifting, conservation and cataloging of ancient mosaics. Each artwork style and period requires the development of dedicated processing methods to take into account a priori information of materials, shape, color, etc. An interesting point of view

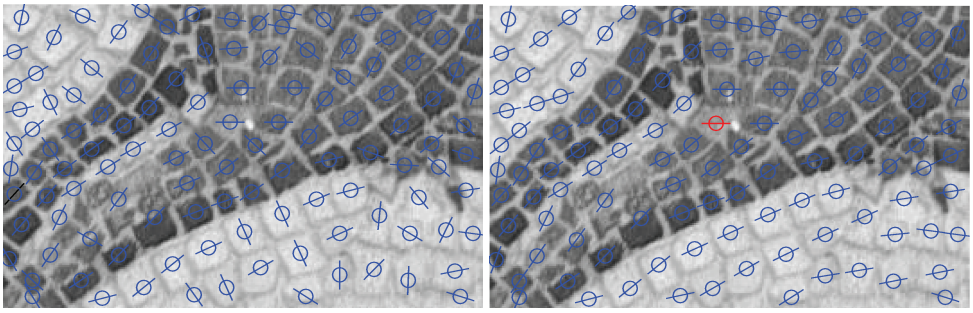

(a) Configuration at initialization (b) Configuration after SA

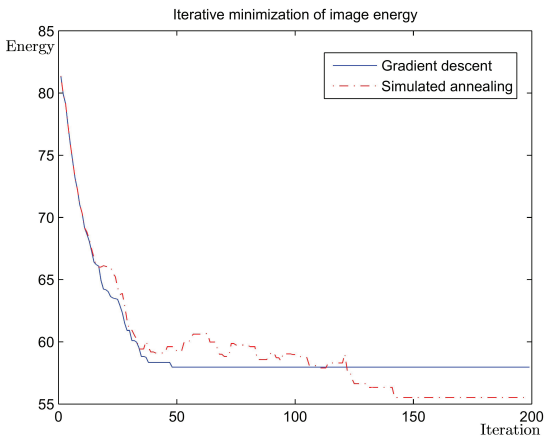

(c) Energy evolution for GD and SA

FIGURE 16.16
Cartography of tesserae orientation. Each tessera is characterized by its center of mass (circle) and its orientation (segment crossing the circle).

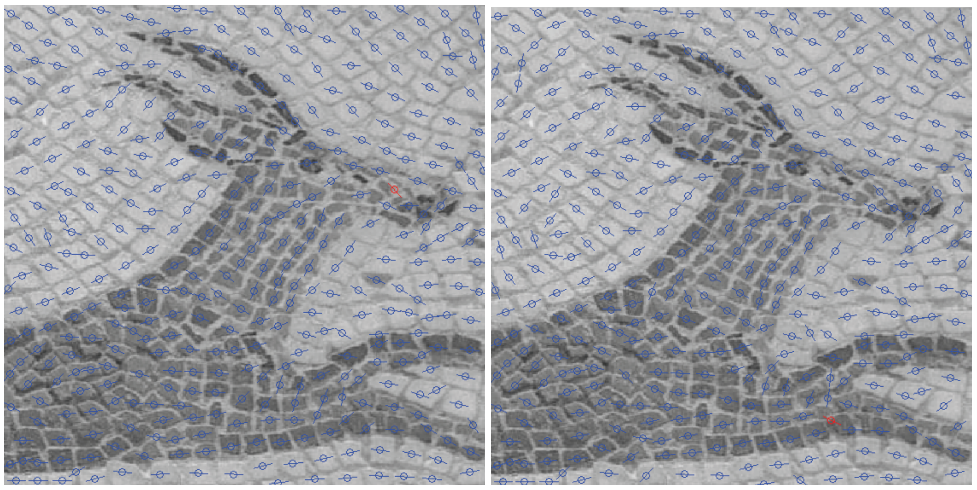

(a) Configuration after SA (b) Configuration after GD

FIGURE 16.17
Another example of tesserae orientation cartography with (a) simulated annealing optimization and (b) gradient descent optimization.

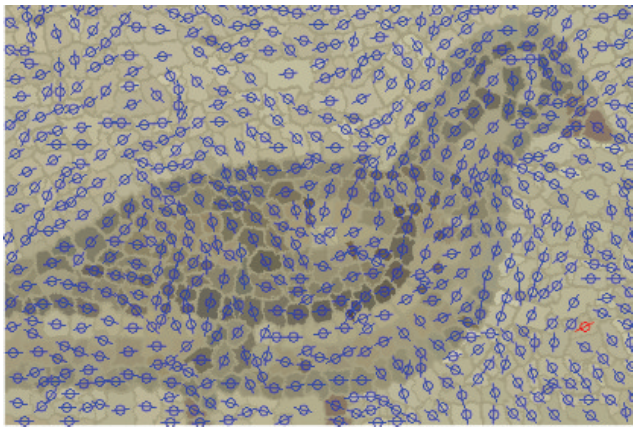

FIGURE 16.18
Result of guidelines detection for the "bird" mosaic in Figure 16.12(a).

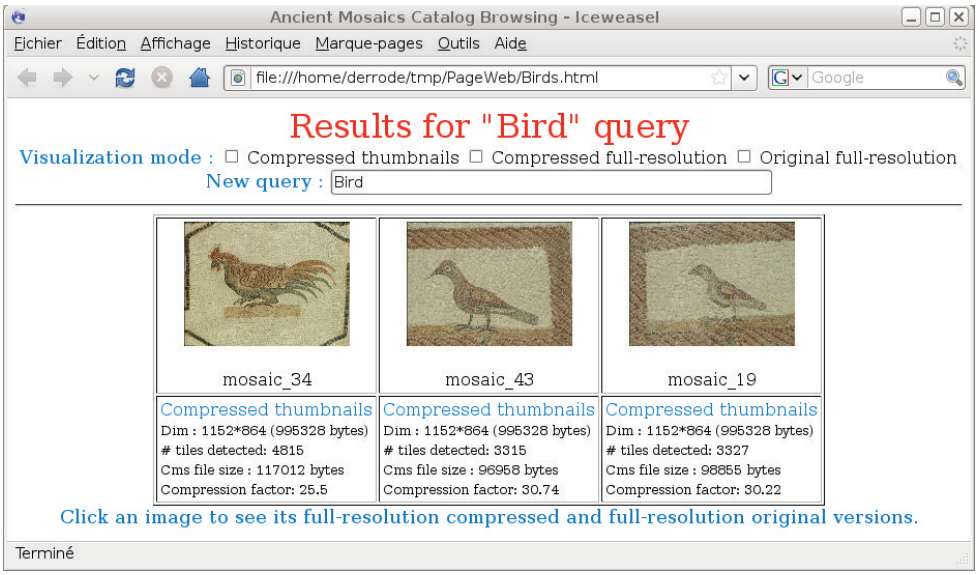

FIGURE 16.19
Example of querying a distant mosaic catalog by keyword.

on the problem is to consider, within the processings, that a mosaic is a collection of tiles and not only a series of image pixels. If this tessera-oriented strategy seems suited in numerous cases, improvement regarding the robustness of tesserae extraction are still required, especially when mosaic tiles show a large difference in size and a high level of degradation.

The algorithms described within Sections 16.3 to 16.5 are only a few basic, but crucial, steps toward complete applications expected by experts such as (i) ancient mosaic restoration with virtual "inpainting" tools taking into account main guidelines and tesserae shapes, and (ii) multi-site and distant catalog browsing with "intelligent" retrieval capabilities of semantic objects. A simple `html` interface has been designed to illustrate the possible use of basic modules for browsing, *in situ*, a distant database of Roman-style mosaics. A simple query using textual keywords like "human", "face" or "animal" allows to visualize the corresponding mosaics in a distant database. Figure 16.19 shows an example of this application with the word "bird" as query. Of course, one goal of the project is to replace keywords by self-content indexing using semantic objects extraction and characterization, based on segmentation, main guidelines estimation and connected components labeling algorithms [22]. The mosaic coding strategy exposed above can be used to construct a tile-oriented CBIR application. If the CBIR can work directly on the coded stream (without reconstruction), one can expect to reduce drastically the RAM and/or hard disk memory requirements.

The problem of quality of processings for segmentation and lossy coding has not been addressed in this Chapter. Particular attention should be paid to this issue in order to quantify the effectiveness of the approach. To that goal, specific quality metrics for tesserae shape and color have to be defined with experts and evaluated against image resolution. Cumulative error impact should then be analyzed along the complete processing chain to evaluate the level of accuracy for the targeted application. Note that fully automatic tools are not always required and applications piloted by users can be of interest.

An interesting open issue is the construction of an invariant representation of semantic mosaic objects which is robust to the tiling organisation of shapes. Such a module will help CBIR systems to retrieve mosaic

objects independently of their orientation, pose and size in the scenes. Dedicated registration algorithms to reconstruct a complete mosaic scene from a set of sub-images can also be of interest in case of *in situ* acquisition of a large mosaic for example.

Finally, one very promising research direction is to develop new image processing methods to automatically learn ancient mosaicists' way of working and style (e.g., tessera color and size, organisation, guidelines, etc.). These tools could first be used to virtually fill in missing patches or restore deteriorated patches in a mosaic scene, using tessera-dedicated inpainting methods. They could also be exploited for emulating a mosaic artwork style from a raster input image using computer-aided algorithms, *cf.* [6] for an overview of digital mosaic creation.

Bibliography

[1] http://www.americanmosaics.org/, Last visit on Apr. 2010. The Society of American Mosaic Artists.

[2] http://www.bamm.org.uk/, Last visit on Apr. 2010. The British Association for Modern Mosaic.

[3] http://www.getty.edu/conservation/, Last visit on Apr. 2010. The Getty Conservation Institute.

[4] http://zoi.utia.cas.cz/mosaic.html, Last visit on Apr. 2010. Institute of Information Theory and Automation, Academy of Sciences of the Czech Republic.

[5] S. Battiato, G. Di Blasi, G. M. Farinella, and G. Gallo. A novel technique for Opus Vermiculatum mosaic rendering. In *Proc. of the 14th Int. Conf. on Computer Graphics, Visualization and Computer Vision (WSCG'06)*, Plzen, Czech Republic, 2006.

[6] S. Battiato, G. Di Blasi, G. M. Farinella, and G. Gallo. Digital mosaic frameworks: an overview. *Computer Graphic Forum*, 26(4):794–812, December 2007.

[7] A. Baumgartner, S. Hinz, and C. Wiedemann. Efficient methods and interfaces for road tracking. In *Photogrammetric Computer Vision (PCV'02)*, page B:28, Graz, Austria, 2002.

[8] L. Benyoussef and S. Derrode. Tessella-oriented segmentation and guideline estimation of ancient mosaic images. *J. of Electronic Imaging*, 17(4), 2008.

[9] L. Benyoussef and S. Derrode. Représentation orientée tesselle d'images de mosaiques anciennes. In *GRETSI'09*, Dijon, France, 8-11 September 2009.

[10] Cristina Boschettia, Cristina Leonellib, Michele Macchiarolac, Paolo Veronesiband Anna Corradib, and Cinzia Sada. Early evidences of vitreous materials in Roman mosaics from Italy: An archaeological and archaeometric integrated study. *Journal of Cultural Heritage*, 9(sup. 1):e21–e26, 2008.

[11] P. Bruneau. *La mosaïque antique*. Presses de l'université de Paris-Sorbonne, 1987.

[12] A. C. S. Chung. Image segmentation methods for detecting blood vessels in angiography. In *IEEE Int. Conf. on Automation, Robotics and Computer Vision (ICARCV'06)*, pages 1–6, Singapore, 2006.

[13] S. Derrode and F. Ghorbel. Robust and efficient Fourier-Mellin transform approximations for invariant grey-level image description and reconstruction. *Computer Vision and Image Understanding*, 83(1):57–78, 2001.

[14] M. O. Djibril and R. O. H. Thami. Islamic geometrical patterns indexing and classification using discrete symmetry groups. *Journal on Computing and Cultural Heritage*, 1(2):1–14, 2008.

[15] M. O. Djibril, R. O. H. Thami, R. Benslimane, and M. Daoudi. Une nouvelle technique pour l'indexation des arabesques basée sur la dimension fractale. In *Compression et Représentation des Signaux Audiovisuels (CORESA'05)*, Rennes, France, 2005.

[16] K. M. D. Dunbain. *Mosaics of the Greek and Roman world*. Cambridge University Press, 1999.

[17] Cesare Fiori, Mariangela Vandini, Silvia Prati, and Giuseppe Chiavari. Vaterite in the mortars of a mosaic in the Saint Peter basilica, Vatican (Rome). *Journal of Cultural Heritage*, 10(2):248–257, 2009.

[18] M. A. Fischler, J. M. Tenenbaum, and H. C. Wolf. Detection of road and linear structures in low resolution aerial images using multi-source knowledge integration techniques. *Computer Graphics and Image Processing*, 15(3):201–223, 1981.

[19] T. Géraud and J. B. Mouret. Fast road network extraction in satellite images using mathematical morphology and Markov random fields. *EURASIP Journal on Applied Signal Processing*, 2004(16):2503–2514, 2004.

[20] F. Ghorbel. A complete invariant description for gray-level images by the harmonic analysis approach. *Pattern Recognition Letters*, 15:1043–1051, 1994.

[21] F. A. Gil, J. M. Gomis, and M. Pérez. Reconstruction techniques for image analysis of ancient islamic mosaics. *Int. Journal of Virtual Reality*, 8(3):5–12, 2009.

[22] R. C. Gonzalez and R. E. Woods. *Digital Image Processing*. Addison-Wesley Publishing Company, 1992.

[23] R. Kadobayashi, N. Kochi, H. Otani, and R. Furukawa. Comparison and evaluation of laser scanning and photogrammetry and their combined use for digital recording of Cultural Heritage. In *Proc. of the ISPRS Congress*, Istanbul, Turkey, 2004.

[24] S. Kirkpatrick, C. D. Gelatt, and M. P. Vecchi. Optimization by simulated annealing. *Science, New Series*, 220(4598):671–680, May 1983.

[25] P. Kratochvil. Greek mosaic from paphos, cyprus, Last visit on Apr. 2010. http://www.publicdomainpictures.net/view-image.php?image=4512&picture=mosaiques-grecques&large=1.

[26] R.J. Ling. *Ancient Mosaics*. British Musuem, 1998.

[27] W. Maghrebi, L. Baccour, M. A. Khabou, and A. M. Alimi. An indexing and retrieval system of historic art images based on fuzzy shape similarity. In *6th Mexican Int. Conf. on Artificial Intelligence (MICAI 2007)*, pages 623–633, Aguascalientes, Mexico, 2007.

[28] Wafa Maghrebi, Anis Borchani, Mohamed A. Khabou, and Adel M. Alimi. A system for historic document image indexing and retrieval based on XML database conforming to MPEG7 standard. In *7th Int. Workshop on Graphics Recognition. Recent Advances and New Opportunities (GREC'07)*, pages 114–125, Curitiba, Brazil, 2007.

[29] H. Mayer, S. Hinz, U. Bacher, and E. Baltsavias. A test of automatic road extraction approaches. In *Photogrammetric Computer Vision (PCV'06)*, Bonn, Germany, 2006.

[30] J. B. Mena and J. A. Malpica. An automatic method for road extraction in rural and semi-urban areas starting from high resolution satellite imagery. *Pattern Recognition Letters*, 26(9):1201–1220, July 2005.

[31] F. Meyer and S. Beucher. *The Morphological Approach of Segmentation: the Watershed Transformation*, chapter Mathematical Morphology in Image Processing, Dougherty E. Editor. Marcel Dekker, New York, 1992.

[32] M. M'hedhbi, R. Mezhoud, S. M'hiri, and F. Ghorbel. A new content-based image indexing and retrieval system of mosaic images. In *3rd Int. Conf. on Information and Communication Technologies: from Theroy to Applications (ICT-TA'06)*, pages 1715–1719, Damascus, Syria, 24-28 April 2006.

[33] F. Mokhtarian and A. Mackworth. A theory of multiscale, curvature-based shape representation for planar curves. *IEEE Trans. on Pattern Analysis and Machine Intelligence*, 14(8):789–805, 1992.

[34] noname. Mosaics *In Situ* project - illustrated glossary. Technical report [3], The Getty Conservation Institute and the Israel Antiquities Authority, 2003.

[35] Eric Persoon and K.-S. Fu. Shape discrimination using Fourier descriptors. *IEEE trans. On Systems, Man and Cybernetics*, 7(3):170–179, 1977.

[36] M. Rochery, I. H. Jermyn, and J. Zerubia. Higher order active contours. *Int. J. of Computer Vision*, 69(1):27–42, August 2006.

[37] G. Salemi, V. Achilli, M. Ferrarese, and G. Boatto. High resolution morphometric reconstruction of multimaterial tiles of an ancient mosaic. In *Proc. of the ISPRS Congress*, page B5: 303 ff, Beijing, China, 2008.

[38] Carlo Stefano Salerno, Cesare Moretti, Teresa Medici, Teresa Morna, and Marco Verità. Glass weathering in 18th century mosaics: The São João Chapel in the São Roque Church in Lisbon. *Journal of Cultural Heritage*, 9(sup. 1):e37–e40, 2008.

[39] C. Steger. An unbiased detector of curvilinear structures. *IEEE trans. on Image Processing*, 20(2):113–125, February 1998.

[40] F. Tupin, H. Maitre, J. F. Mangin, J. M. Nicolas, and E. Pechersky. Detection of linear features in SAR images: application to road network extraction. *IEEE trans. on Geoscience and Remote Sensing*, 36(2):434–453, 1998.

[41] J. M. Valiente, F. Albert, and J. M. Gomis. A computational model for pattern and tile designs classification using plane symmetry groups. In *Proc. of the Ibero American Congress on Pattern Recognition (CIARP)*, Havana, Cuba, 2005.

[42] C. M. Van Bemmel, L. J. Spreeuwers, M. A. Viergever, and W. J. Niessen. Level-set-based artery-vein separation in blood pool agent CE-MR angiograms. *IEEE trans. on Medical Imaging*, 22:1224–1234, 2003.

[43] L. Vincent. Grayscale area openings and closings: their applications and efficient implementation. In *Proc. EURASIP Workshop on Mathematical Morphology and its Applications to Signal Processing*, pages 22–27, Barcelona, Spain, May 1993.

[44] R. Westgate. Ancient mosaics - a bibliography, Last visit on Apr. 2010. http://www.cardiff.ac.uk/hisar/people/rw/mosaicbibliog.html.

[45] O. Wink, W. Niessen, and M. A. Viergever. Multiscale vessel tracking. *IEEE trans. on Medical Imaging*, 23(1):130–133, 2004.

[46] P. J. Yim, G. Boudewijn, C. Vasbinder, V. B. Ho, and P. L. Choyke. Isosurfaces as deformable models for magnetic resonance angiography. *IEEE trans. on Medical Imaging*, 22(7):875–881, July 2003.

[47] A. Zarghili, N. Gadi, R. Bensliman, and K. Bouatouch. Arabo-Moresque decor image retrieval system based on mosaic representations. *Journal of Cultural Heritage*, 2(2):149–154, 2001.

[48] A. Zarghili, J. Kharroubia, and R. Bensliman. Arabo-Moresque decor images retrieval system based on spatial relationships indexing. *Journal of Cultural Heritage*, 9(3):317–325, 2008.

[49] B. Zitová, J. Flusser, and F. Šroubek. An application of image processing in the medieval mosaic conservation. *Pattern Analalysis and Applications*, 7(1):18–25, 2004.

Index